

Disclaimer/Publisher's Note: The statements, opinions, and data contained in all publications are solely those of the individual author(s) and contributor(s) and not of MDPI and/or the editor(s). MDPI and/or the editor(s) disclaim responsibility for any injury to people or property resulting from any ideas, methods, instructions, or products referred to in the content.

Article

# Xiuyan Jade Waste as Antibacterial Additives for Functional Coatings

Jimei Wang <sup>1</sup>, Xiaoyan Wang <sup>1</sup> and Yang Yang <sup>2,\*</sup>

<sup>1</sup> China Building Materials Academy, Beijing 100024, China

<sup>2</sup> Shenzhen Materials Technologies Co. Ltd, Shenzhen 518108, Guangdong Province, China

\* Correspondence: y.y.live@hotmail.com; Tel.: +86-0755-27656888

**Abstract:** Jade waste is a normal byproduct that makes up much more than the amount of jade extracted. Therefore, recycling jade waste is worth investigating from the point of view of energy conservation. Moreover, it is an environment-friendly material, which is desirable for use in building materials. In this study, Xiuyan jade waste was repurposed as antibacterial additives for building coatings. The powder waste was activated by milling and subsequent annealing. The antibacterial properties of the treated waste were mostly related to the annealing temperatures. Based on the investigations of the phase change and the release of metal ions of a series of samples and their antibacterial activities, the antibacterial mechanism of the treated samples was explored experimentally. The most applicable sample for coatings was finally chosen by considering its pH values and its antibacterial abilities. Antibacterial testing showed that the addition of treated jade waste could enhance the bacterial inhibition rate of building coatings from 60% to 99.9%.

**Keywords:** jade waste; antibacterial agent; activation temperature; coatings

---

## 1. Introduction

A large amount of Xiuyan jade has been exploited in recent years. When mining jade, waste byproduct is produced, which is much more than the amount of jade recovered. Therefore, recycling Xiuyan jade waste is worth investigating from the point of view of energy conservation. Moreover, jade waste is a kind of environment-friendly material that is desirable for building materials. As people become more and more concerned about their health, building materials are to be functionalized to suit improved human health. This is especially true because of the emergence of different viruses and bacteria around the world and their threat to the health of human beings [1]. In this study, Xiuyan jade waste is transformed into a very effective antibacterial agent, which could be used as antibacterial additives in building coatings.

There have been many chemically synthesized antibacterial agents introduced in recent years, such as Ag-based materials including silver nanoparticles, silver nanoparticles–alginate composites, and nanosilver textile materials [2–5]. Similar to copper ions [6–8], Ag ions are positive and very active. The bacteriostatic action mainly originates from the direct interaction of  $\text{Ag}^+/\text{Cu}^{2+}$  species with the cell components. The redox reaction of these ions produces hydroxyl radicals ( $\text{-OH}$ ) and superoxide anions ( $\text{-O}_2^-$ ) when they get in contact with the bacterial surface. Additionally, Ag ions/Cu ions easily attach to bacterial membranes or even enter bacteria, which could severely damage bacteria's structure. Additionally, semiconductor metal oxides [9–11] such as  $\text{TiO}_2$  and  $\text{ZnO}$  are widely used as antibacterial agents. The hydroxyl radicals and superoxide radicals produced when they react under the light are lethal to bacteria. For metal oxides such as  $\text{MgO}$  and  $\text{CaO}$  [12–14], which easily react with water, the produced hydroxyl ions are harmful to the environment of bacteria, and eventually kill them. These antibacterial agents are poisonous to bacteria; however, they may not be friendly to the environment. On the other hand, jade waste is environmentally friendly and can easily be collected from nature, which is much simpler than the chemical synthesis process. Thus, it is worth developing as safe building materials.

In our study, the antibacterial mechanisms of jade waste are explored. The results show that Mg ions and Ca ions could be released when the jade waste is activated at rather low temperatures. The antibacterial mechanisms [15–18] may not be creative; however, the emergence of Mg and Ca ions from the waste is significant for sterilization. As can be seen from previous studies, some mineral wastes have been developed for different uses [19–21]; however, the activation of the waste at rather high temperature is crucial for obtaining good performance of natural minerals. The current study shows that the processes of milling and subsequent annealing at very low temperatures are sufficient to produce the antibacterial ability of the collected Xiuyan jade waste, which is meaningful for its application.

## 2. Experimental

### 2.1. Materials and Methodology

The raw materials taken from Xiuyan jade waste are grounded with a ball grinder (Model TR1114) and filtered using a 1000-mesh sieve. The obtained fine powder is further annealed in air using a resistance furnace (Model 4-10) at temperatures of 270°C, 500°C, 600°C, 700°C, 800°C, and 900°C for 2 h and is labeled as the sample numbers from 1# to 6#, respectively. The unannealed powder sample is numbered as 0#. For some samples annealed under 180°C, 350°C and 400°C for 2h, they are not numbered.

The powder X-ray diffraction patterns of all specimens were obtained using X-ray diffraction analysis (XRD, Rigaku-MiniFlex600) with Cu K $\alpha$  radiation ( $\lambda = 1.5406 \text{ \AA}$ ) as the source. The step size was 0.02° and the scan rate was set to 3°/min.

### 2.2 Metal leaching test and pH value

A total of 0.1 g of each sample was taken and dissolved in 100 mL of standard water. Thorough stirring was necessary to obtain a homogenous solution. The well-mixed solution was then ready for pH value measurement. For the metal leaching test, the homogenous solution was further centrifuged at 8000 rad/min for 30 min. The supernatant was then taken out and filtered using membranes with a pore size of 0.22  $\mu\text{m}$ . An inductively coupled plasma atomic emission spectrometer was employed for testing the elements of Mg, Al, and Ca.

### 2.3 Zeta Potential

0.1 g of each powdered sample was mixed with a 100 mL of distilled water and stored for 24 h. The mixture was centrifuged for 5 min at a speed of 1500 rad/min, and the supernatant was used for the measurement. The Zeta potentials of the solution were measured as a function of the solid-to-liquid ratio using a Zeta-potential meter (Malvern Nano-ZS/ZEN-3600, UK).

### 2.4 Bactericidal Test

The antibacterial efficacy of all specimens was ascertained using a procedure adopted from a standard testing method, that is, QBT 2738-2012.

To calculate the percentage of antibacterial efficacy, Equation (1) is used:

$$\text{Percentage of antibacterial efficacy (\%)} = \frac{I - II}{I} \times 100, \quad (1)$$

where  $I$  is the count of test microorganisms recovered from the inoculated reference sample without Xiuyan jade waste (cfu/mL), and  $II$  is count of test microorganisms recovered from the inoculated sample with Xiuyan jade waste (cfu/mL).

Before the test, the powdered materials should first be diluted in sterile standard hard water to a concentration of 5 and 25 g/L in our work.

The bactericidal tests were carried out using *Escherichia coli* (ATCC25922) or *Staphylococcus aureus* (ATCC6538) as the testing strains. The contact time of the bacterial suspension on the testing materials is also critical to the antibacterial efficacy. Different times were set to find the optimal antibacterial efficacy of the testing materials.

### 3. Results and Discussion

First, the antibacterial efficacy of all samples was measured with a 5 g/L concentration of powdered materials and at a contact time of 2 h. The results are listed in Table 1.

**Table 1.** Antibacterial deduction (%) of Xiuyan jade waste (5 g/L, 2 h).

Samples Strains	0#	1#	2#	3#	4#	5#	6#
Escherichia coli (ATCC25922)	0	37	22	73	93	98	100
Staphylococcus aureus (ATCC6538)	0	53	44	71	91	96	100

There is an obvious trend of increasing antibacterial activity of the Xiuyan jade waste along with the increase in annealing temperatures. For the sample annealed at 900°C, all the bacterial strains could be killed within 2 h. When the contact time was shortened to 30 min or 10 min, the antibacterial efficacy remained at 100%. Overall, Xiuyan jade waste after 900°C annealing showed quick sterilizing ability; it can kill bacteria within 5–10 min, as shown in Table 2. The results show that Xiuyan jade waste could be used as a kind of antibacterial material with very effective antibacterial efficacy. Based on the excellent antibacterial performance, more studies are necessary to learn about the jade waste's antibacterial mechanism.

**Table 2.** Antibacterial deduction (%) of sample 9# (5 g/L, variable contact time).

Contact time Strains	5 min	10 min	30 min	2 h
Escherichia coli (ATCC25922)	49	100	100	100
Staphylococcus aureus (ATCC6538)	44	100	100	100

The phase change exhibited by Xiuyan jade waste when annealed at different temperatures was obtained using XRD. The XRD patterns of samples 0# and 1# are almost identical, indicating that there was no obvious phase change after annealing at 270°C. The XRD patterns for the raw materials of Xiuyan jade waste are complicated, as shown in Figure 1. Seven types of minerals could be detected from the XRD patterns of samples and the possible content of different minerals is listed in the inset table.

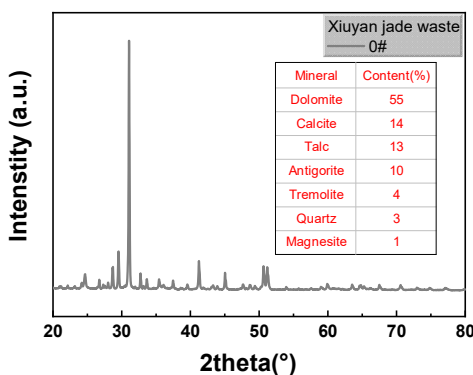


**Figure 1.** XRD pattern of the original Xiuyan jade waste.

By increasing the annealing temperature of the Xiuyan jade waste to 500°C or higher, two peaks appeared and are related to magnesite, corresponding to 32.2° and 53.9°, respectively, which get weaker and weaker. When the annealing temperature reached 600°C, the peaks almost disappear. As

the annealing temperature increased to 700°C, another main peak of antigorite at 24.6° gradually disappeared. Meanwhile, two main peaks of MgO appear, corresponding to 43.0° and 62.0°, respectively. Note that when the annealing temperature is around 700°C, only a few CaO could be observed using XRD. Whereas, when the annealing temperature of the Xiuyan jade waste increased to 800°, the main peaks of dolomite at 41.2° and talc at 30.9° decreased considerably. Additionally, part of the calcite phase changed, resulting in an intensive increase of CaO when the annealing temperature changed from 700°C to 800°C. At the same time, a new phase of calcium hydroxide related to the peak at 34.2° started to appear. As the annealing temperature was further increased to 900°C, the phase of the dolomite decreased while the peaks of calcium hydroxide  $\text{Ca}(\text{OH})_2$  was largely enhanced, accompanied by the disappearance of the main peaks of CaO at 37.4° and calcite at 29.5°. To show more detail about the phase change caused by the different annealing temperatures, the comparisons between each XRD pattern are presented separately, as shown in Figures 2(a-d).

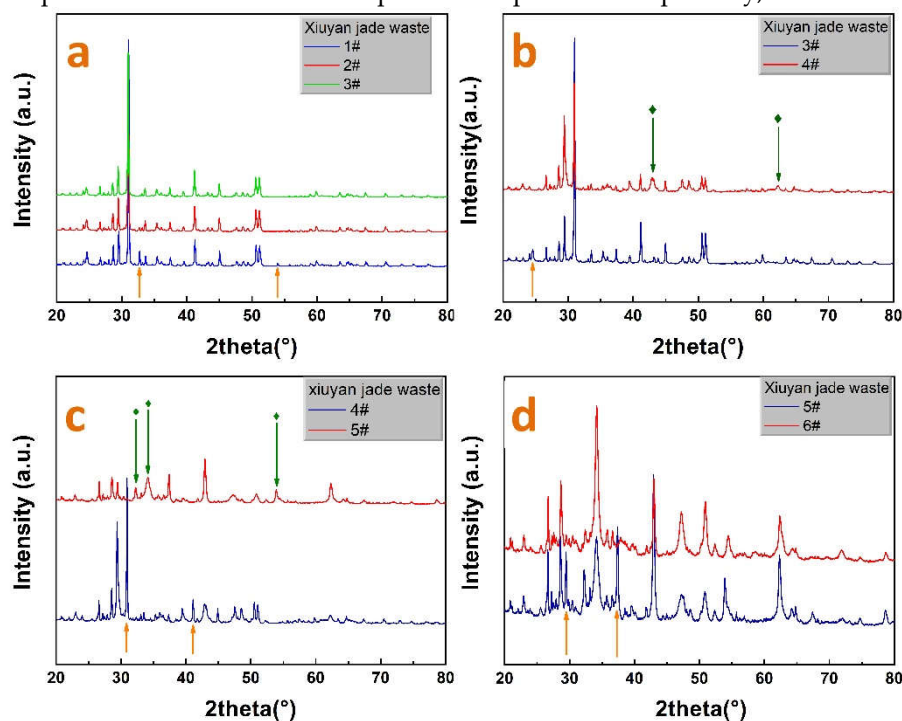


**Figure 2.** XRD patterns for the observation of phase changes.

Based on the XRD patterns, the phase changes could be observed clearly. When the annealing temperature increased from 270°C to 900°C, the minerals involved decomposed gradually, and finally turned into  $\text{SiO}_2$ , MgO, and  $\text{Ca}(\text{OH})_2$ . These changes were also evidenced by the measured pH values. As the annealing temperatures increase, the content of alkaline oxides in the annealed products also increases, resulting in enhanced pH values. Although sample 6# shows the best antibacterial ability, its pH value of 12.5 is also the highest, which is not suitable for coating additives [22]. Usually, samples with pH values lower than 9.5 are optional for antibacterial coatings.

As indicated by XRD analysis, the Xiuyan jade waste is relatively steady when annealed at temperatures below 500°C. However, there are some obvious differences in the antibacterial activities when the samples are annealed at 180°C, 270°C, 350°C, 400°C, and 500°C. To throw more light on these questions, more details on the release of metal ions and Zeta potentials have been investigated.

For each sample, 0.05, 0.1, and 20 g of powders were dissolved in distilled water and kept for 24 h. There were three recorded dots from left to right corresponding to each activation temperature, as indicated by the arrows in the plot (Figure 3). For the samples annealed below 500°C, with the increase of used powders from 0.05 to 20 g, the released Mg ions increases clearly, while the amount of released Ca ions shows different trends. The Ca ions decreased obviously, when the amount of used powders increased to 20 g. when excessive powders were dissolved into the solution, there seems to be a competition between the released Mg and Ca ions. For the samples annealed at 500°C

or higher, Ca ions seem more competitive, as the amount of released Ca ions could reach over 100 mg/L. On the other hand, the amount of Mg ions stays below 0.05 or less. For the samples annealed at 800°C and 900°C, the released Ca ions could reach over 1000 mg/L (which are not included in the plot), while the amounts of Mg ions are rather low, around 0.02 and 0.01 mg/L, respectively. Note that with the increase of used powder in 100 mL distilled water, the released ions also increased. However, the increase rates for Ca and Mg ions are different. When the dosage of powder varied from 0.05 to 0.1 g, the Ca ions increase from 5.2 to 5.42 mg/L for the sample activated at 270°C, while the Mg ions increase from 0.53 to 0.81 mg/L. In this case, Mg ions seem to be more competitive. However, this trend changed significantly for the sample activated above 500°C. For example, when the amount of powder samples varied from 0.05 to 0.1 g, the Ca ions increase from 103.6 to 220.8 mg/L for the sample activated at 900°C, while the Mg ions increase from 1.32 to 1.15 mg/L.

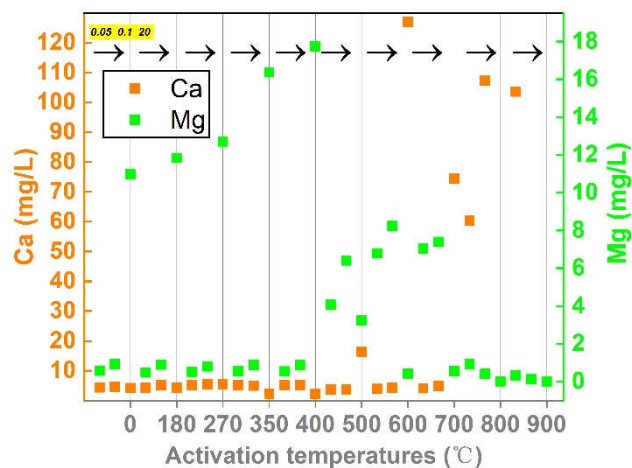
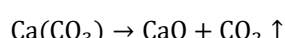


**Figure 3.** Released metal ions when 0.05-, 0.1-, and 20-g powder samples are separately dissolved into 100-ml DI water.

As shown by the XRD analysis, 500°C is a critical temperature for phase change; the reaction is as follows:



When the annealing temperature reaches between 700°C and 800°C,  $\text{Ca}(\text{CO}_3)$  starts to decompose as follows:



However, the produced  $\text{CaO}$  is not stable and easily reacts with water, resulting in the generation of  $\text{Ca}(\text{OH})_2$ .

Based on the reactions [23,24] just mentioned, the released Ca and Mg ions are related to the phases in the jade waste. This depends on the solubility of the phases in distilled water, which is the solvent used in the measurement.  $\text{MgO}$  is converted to  $\text{Mg}(\text{OH})_2$  when the jade waste annealed above 500°C is dissolved in water. Therefore, less Mg ions can be released than the one annealed under 500°C because the solubility of  $\text{Mg}(\text{OH})_2$  is less than that of  $\text{MgCO}_3$ . Similarly, there will be more Ca ions released when  $\text{Ca}(\text{CO}_3)$  is converted to  $\text{CaO}$  or even  $\text{Ca}(\text{OH})_2$  because the solubility of  $\text{Ca}(\text{OH})_2$  is higher than that of  $\text{Ca}(\text{CO}_3)$ .

As analyzed from the results, for the samples annealed below 500°C, the released ions are directly from the mineral phases rather than from the metal oxides. The concentration of powder waste is not really important to its antibacterial performance because even when the amount of powder is as high as 20 g, the released ions are still not as high as expected; that is, the ratio of the released ions to the amount of used powders are the least in the experiment. These results help a lot in our understanding of the antibacterial performance of jade waste.

Based on the bactericidal tests, when the jade waste was annealed below 270°C, the samples showed excellent antibacterial activity. As evident from previous reports,  $\text{Mg}^{2+}$  and  $\text{Ca}^{2+}$  ions possess antibacterial activity, and  $\text{Mg}^{2+}$  ions are more active than  $\text{Ca}^{2+}$  [25], generally. The amount of metal ions released from the studied jade waste was only slightly different among samples annealed under

500°C; however, Zeta potential measurement indicated that their surface charges were largely different from each other. pH values of the compared samples (0°C, 180°C, 270°C, 350°C, and 400°C) were similar ( $\sim 8.0$ ), and their Zeta potentials were recorded and shown in Figure 4. The absolute value for the Zeta potential of the sample annealed under 270°C was the highest, indicating that the surface charges of the particles in the powder–water solution are the most stable. This might be an important factor in influencing the attachment of the released cations onto the bacterial cells [26–28], thereby contributing to the antibacterial ability.

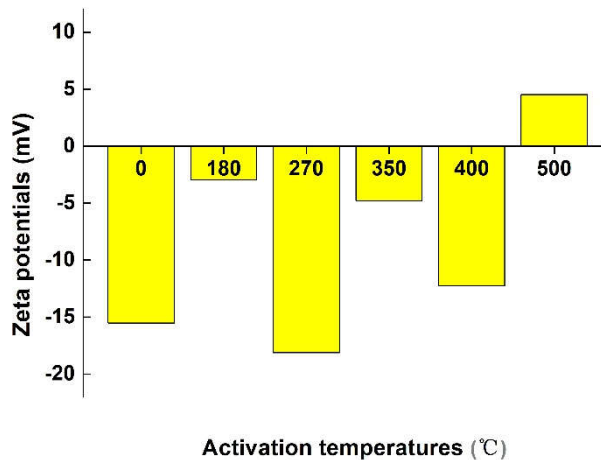


**Figure 4.** Zeta potentials when jade waste powders (0.5 g) are dissolved into 100-ml DI water.

The morphologies of the broken bacterial cells observed using TEM are shown in Figures 5a and 5b. The images on the left of the arrow are the integrated cells with perfect shapes for *E. coli* and *S. aureus*. After contacting the jade waste activated at 270°C for 2h, extreme damages such as the broken of cell wall and the leakage of the cellular contents are observed in these microorganisms.

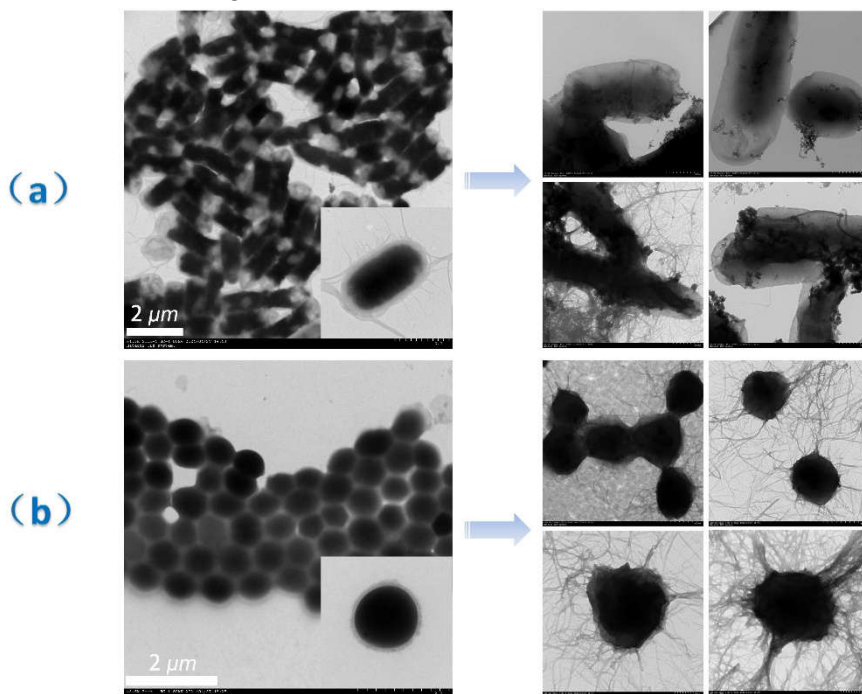


**Figure 5.** Morphologies of (a) *E. coli* and (b) *S. aureus* cells when contacted with jade waste (sample 2#) for 2 h.

When considering the application of jade waste in building materials, the antibacterial activity of samples 1# and 2# were further studied based on different testing conditions because of their much

lower pH values (Table 3). The commonly used concentration of jade waste in bactericidal tests was 5 g/L, when the concentration was increased to 25 g/L, the antibacterial effect changed little.

**Table 3.** pH values of the powder-water solution (0.1%).

Samples	0#	1#	2#	3#	4#	5#	6#
pH values	7.8	8.0	10.3	10.5	11.9	12.6	12.6

Note: The pH values of samples annealed at the temperatures of 180°C, 270°C, 350°C, and 400°C are almost the same, approximately 8.0 ± 0.2.

As indicated in Table 4, an obvious phenomenon could be observed. The antibacterial efficiency of Xiuyan jade waste is much more dependent on the contact time during the test, while it is much less related to the concentration of antibacterial suspensions. When the contact time reached 24 h, the antibacterial efficiency of samples 1# and 2# could be above 99%. Therefore, these samples are very suitable options as additions for antibacterial coatings.

**Table 4.** Antibacterial deduction (%) for different testing conditions.

Testing conditions	5 g/L 2 h	5 g/L 24 h	25 g/L 2 h	5 g/L 2 h	5 g/L 24 h	25 g/L 2 h
Strains	<i>E. coli</i> (ATCC25922)			<i>S. Aureus</i> ( ATCC6538)		
1#	37	99.6	38	53	99.6	33
2#	22	99.9	35	44	99.9	35

### 3.1 Application in Antibacterial Coatings

Jade waste, one kind of architectural interior coating was used as the base. Sample 1# was chosen because of its moderate pH value and its remarkable antibacterial properties. The proportion of additive was 5% in weight. The antibacterial activities were monitored based on the testing standard of HG/T 3950-2012 (antibacterial coating). There was a significant difference in the antibacterial activities observed between the coatings with and without the addition of jade waste. The antibacterial efficacy of the original coating is only 55%–65% for *E. coli* and *S. Aureus*, while the antibacterial efficacy was enhanced to higher than 99.9% with the addition of jade waste.

### 3.2 Outstanding Antibacterial Performance for Application

The application properties of the antibacterial coatings were further determined based on the national standards GB/T 9756-2018 (synthetic resin emulsion coatings for interior wall) and GB 18582-2020 (Limit of harmful substance of architectural coatings). The details are shown in Table 5. According to the results, jade waste plays an important role in the outstanding antibacterial performance of the coatings, which could also meet the requirements for superior products of various standards for application.

**Table 5.** Application properties of the antibacterial coatings.

Items	Results	Conclusion
Application condition	The mixed coatings are homogeneous without any lumps	Qualified
Constructability	Easy to finish twice brushwork	Qualified
Stability at ambient temperature	Not metamorphic	Qualified
Surface drying time	55 minutes	Qualified
Alkali resistance	No abnormalities	Qualified
Contract ratio	0.95	Qualified
Scrub resistance	6000 times	Qualified
Content of volatile organic compound	38.7 g/L	Qualified
Note: Benzene, methylbenzene, ethylbenzene, xylene, free formaldehyde, and heavy metals (including Pb, Cr, Cd, and Hg) are not detectable in the coatings.		

#### 4. Conclusions

In this study, jade waste was repurposed as an antibacterial agent. First, the pH values and the antibacterial activity of jade waste were investigated as a function of activation temperatures. Because of the existence of MgO and CaO for samples annealed above 500°C, the pH value of jade waste was much higher than that annealed below 500°C. The jade waste activated under 900°C possesses the most effective antibacterial activity because of its strong alkalinity. A low activation temperature of 270°C is optimal because the pH value of jade waste is very low and its antibacterial activity is good enough for application as an antibacterial agent. When 5% jade waste was added into interior coatings, the antibacterial efficiency was enhanced from 50%–60% to above 99.9% against Gram-positive and Gram-negative bacteria.

**Author Contributions:** Methodology, Wang X. Y.; Formal Analysis, Wang X. Y.; Investigation, Wang X. Y. and Wang J. M.; Resources, Wang J. M.; Writing – Original Draft Preparation, Wang J. M.; Writing – Review & Editing, Yang Y.; Project Administration, Wang J. M. and Yang Y. All the authors have read and agreed to the published version of the manuscript.

**Funding:** This research was funded by Innovation Commission of Shenzhen grant number [JCYJ20190808154613434].

**Institutional Review Board Statement:** Not applicable.

**Informed Consent Statement:** Not applicable.

**Data Availability Statement:** Data are contained within the article.

**Conflicts of Interest:** The authors declare no conflict of interest.

#### References

- [1] Wang L.J.; Guo X.D.; Zhang H.M.; Liu Y.X.; Wang Y. X.; Liu K.; Liang H.F.; Ming W.Y. Recent advances in superhydrophobic and antibacterial coatings for biomedical materials. *Coatings* 2022, 12, 1469.
- [2] Gawlik-Maj, M.; Babczyńska, A.; Gerber, H.; Kotuła, J.; Sobieszczańska, B.; Sarul, M. Cytotoxicity of Silver-Containing Coatings Used in Dentistry, a Systematic Review. *Coatings* 2022, 12, 1338.

[3] Ren, Y.; Fan, T.Y.; Wang, X.N.; Guan, Y.Y.; Zhou, L.; Cui, L.; Li, M.X.; Zhang, G.Y. In Situ Reduction of Silver Nanoparticles on the Plasma-Induced Chitosan Grafted Polylactic Acid Nonwoven Fabrics for Improvement of Antibacterial Activity. *Coatings* 2021, 11, 1517.

[4] Xia Y.J.; Jiang X.Y.; Zhang J.; Lin M.; Tang X.S.; Zhang J. ; Liu H.J. Synthesis and characterization of antimicrobial nanosilver/diatomite nanocomposites and its water treatment application. *Appl. Surf. Sci.* 2017, 396, 1760–1764.

[5] Chernousova S.; Epple M. Silver as Antibacterial Agent: Ion, Nanoparticle, and Metal. *Angew. Chem. Int. Ed.* 2013, 52, 1636 –1653.

[6] Kozlowski H.; Janicka-Klos A.; Brasun J. Gaggelli E.; Valensin D.; Valensin G. Copper, iron, and zinc ions homeostasis and their role in neurodegenerative disorders (metal uptake, transport, distribution and regulation) *Coordin. Chem. Rev.* 2009, 253, 2665–2685.

[7] Behrang, S.; Sedláček, I.; Štěrba, J.; Suková, G.; Czigány, Z.; Buršíková, V.; Souček, P.; Sochora, V.; Balázs, K.; Vašina, P. An Assessment of the Bactericidal and Virucidal Properties of ZrN-Cu Nanostructured Coatings Deposited by an Industrial PVD System. *Coatings* 2022, 12, 1330.

[8] Wang F.; Yao J.; Si Y.; Chen H.L.; Russel M.; Chen K.; Qian Y.G.; Zaray G.; Bramanti E. Short-time effect of heavy metals upon microbial community activity. *J. Hazard. Mater.* 2010, 173, 510–516.

[9] Raghunath A.; Perumal E. Metal oxide nanoparticles as antimicrobial agents: a promise for the future. *Int. J. Antimicrob. Ag.* 2017, 49, 137–152.

[10] Tsikourkitoudi V.; Henriques-Normark B.; Sotiriou A. G. Inorganic nanoparticle engineering against bacterial infections, *Curr. Opin. Chem. Engin.* 2022, 38, 100872.

[11] Verdier, T.; Bertron, A.; Erable, B.; Roques, C. Bacterial Biofilm Characterization and Microscopic Evaluation of the Antibacterial Properties of a Photocatalytic Coating Protecting Building Material. *Coatings* 2018, 8, 93.

[12] Demirci S.; Yıldırım B.K.,; Tünçay M.M.; Kaya N.; Güllüoğlu A.N. Synthesis, characterization, thermal, and antibacterial activity studies on MgO powders. *J. Sol-Gel Sci. Techn.* 2021, 99, 576–588.

[13] Sawai J.; Yoshikawa T. Quantitative evaluation of antifungal activity of metallic oxide powders (MgO, CaO and ZnO) by an indirect conductimetric assay. *J. Appl. Microbiol.* 2004, 96, 803–809.

[14] Yamamoto O.; Ohira T.; Alvarez K.; Fukuda M. Antibacterial characteristics of CaCO<sub>3</sub>–MgO composites. *Mater. Sci. Eng. B* 2010, 173, 208–212.

[15] Meghana S.; Kabra P.; Chakraborty S.; Padmavathy N. Understanding the pathway of antibacterial activity of copper oxide nanoparticles. *RSC Adv.* 2015, 5, 12293.

[16] Pan X.H.; Wang Y.H.; Chen Z.; Pan D.M.; Cheng Y.J.; Liu Z.J.; Lin Z.; Guan X. Investigation of Antibacterial Activity and Related Mechanism of a Series of Nano-Mg(OH)<sub>2</sub>. *ACS Appl. Mater. Interfaces* 2013, 5, 1137–1142.

[17] Bhattacharya P.; Dey A.; Neogi S. An insight into the mechanism of antibacterial activity by magnesium oxide nanoparticles. *J. Mater. Chem. B* 2021, 9, 5329.

[18] Chaturvedi C.U.; Shrivastava R. Interaction of viral proteins with metal ions: role in maintaining the structure and functions of viruses. *FEMS Immunol. Med. Microbiol.* 2005, 43, 105–114.

[19] Sun S.S.; Zhang Y.M. Preparation of Transparent Glass-ceramics Based on Xiuyan Jade Waste. *J. Shenyang Univ. Chem. Techn.* 2010, 24(1), 44–47.

[20] Hou M.Y. Preparation and Properties of Alkali Activated Slag-based Foam Concrete. Master Thesis, Shandong University of Science and Technology, China, Jun 3, 2020.

[21] Zhang N. Effect of Content of Calcium and Magnesium on the Properties and Structure of Simulated-slag Powders and Their Alkaliactivated Products. Master Thesis, Guangxi University, China, Jul 11, 2020.

[22] Xu F.; Zou H.Z. Techniques and Applications of Building Coatings. 1<sup>st</sup> ed.; China Building Industry Press: Beijing, China, 2009; pp.88–97.

[23] Huang Q.; Wei K.; Xia H.D. A novel perspective of dolomite decomposition: Elementary reactions analysis by thermogravimetric mass spectrometry. *Thermochim. Acta* 2019, 676, 47–51.

[24] Fang Q.; Zhang H.; Guo Y. Thermal Decomposition of Dolomite. *Adv. Mater. Res.* 2010, 177, 617–619.

[25] Wang X.L. Study on antibacterial activity and mechanism of metal ions. Master Thesis, South China University of Technology, China, Apr 20, 2015.

[26] Wyness A.J.; Paterson D.M.; Defew E.C.; Stutter M.I.; Avery L M. The role of zeta potential in the adhesion of *E. coli* to suspended intertidal sediments. *Water Res.* 2018, 142, 159–166.

[27] Bundeleva I.A.; Shirokova L.S.; Pascale Bénézeth P.; Pokrovsky O.S.; Kompantseva E.I.; Balor S. Zeta potential of anoxygenic phototrophic bacteria and Ca adsorption at the cell surface: Possible implications for cell protection from CaCO<sub>3</sub> precipitation in alkaline solutions. *J. Colloid Interf. Sci.* 2011, 360(1), 100–109.

[28] Tang H.M.; Liu Z.S.; Hu B.L.; Zhu L.Z. Effects of iron mineral adhesion on bacterial conjugation: Interfering the transmission of antibiotic resistance genes through an interfacial process. *J. Haz. Mater.* 2022, 435(5), 128889.